Cell Tissue Res (2012) 350:373–384
DOI 10.1007/s00441-012-1481-x

REGULAR ARTICLE

Cochlin expression in vestibular endorgans obtained from patients with Meniere's disease

Audrey P. Calzada · Ivan A. Lopez · Luis Beltran Parrazal · Akira Ishiyama · Gail Ishiyama

Received: 15 April 2012 / Accepted: 10 July 2012 / Published online: 20 September 2012

Abstract The distribution of cochlin and its associated basement membrane proteins (collagen IV, collagen II, laminin-β2, and nidogen-1) were evaluated in the vestibular endorgans of subjects with Meniere's disease and compared with normal specimens. Cochlin mRNA expression in vestibular endorgans from Meniere's disease specimens was also investigated. Specimens were obtained from patients who had Meniere's disease and who were undergoing ablative labyrinthectomy. Control specimens were obtained both from autopsy specimens with documented normal audiovestibular function and from patients undergoing labyrinthectomy for acoustic neuroma excision. In the normal control specimens, cochlin immunoreactivity was found evenly distributed in the stroma of the cristae ampullaris and maculae of the utricle. In Meniere's specimens, cochlin immunoreactivity was markedly increased; this was associated with an increase in cochlin mRNA expression as shown by real-time reverse transcription with the polymerase chain reaction. Collagen IV and laminin-β2 immunoreactivity was significantly decreased in Meniere's specimens. Nidogen-1 and collagen II immunoreactivity was unchanged in Meniere's specimens when compared with normal samples. Cochlin upregulation has been implicated in the hereditary audiovestibulopathy, DFNA9. The increased expression of cochlin and decreased expression of collagen IV and laminin in Meniere's disease are suggestive that the overexpression of cochlin contributes to the dysfunctional inner ear homeostasis seen in this disease.

Keywords Cochlin · Basement membrane · Meniere's disease · Inner ear · Vestibular endorgans · Human

Meniere's disease also known as Menière's or Ménière's disease.

This work was supported by National Institutes of Health grant 5U24 DC 008635 (NIDCD).

A. P. Calzada · I. A. Lopez · A. Ishiyama
Department of Head and Neck Surgery,
UCLA School of Medicine David Geffen,
10833 Le Conte Avenue,
Los Angeles, CA 90095, USA

L. Beltran Parrazal
Center of Cerebral Investigation, Veracruzana University,
Veracruz, Mexico

G. Ishiyama
Neurology Department, UCLA School of Medicine David Geffen,
10833 Le Conte Avenue,
Los Angeles, CA 90095, USA

G. Ishiyama (✉)
UCLA Department of Neurology,
Reed Neurological Research Center at UCLA,
Box 951769, 710 Westwood Blvd.,
Los Angeles CA 90095, USA
e-mail: gishiyama@mednet.ucla.edu

Introduction

Meniere's disease (MD) consists of episodic vertigo, fluctuating sensorineural hearing loss (SNHL), and tinnitus accompanied by a sensation of aural fullness (Baloh 2001). Episodes are known to precipitate from factors such as emotional stress, hormonal fluctuations, and salt intake; patients have fluctuating SNHL that progresses throughout their life, and they experience a significant decrease in physical and psychosocial quality of life (Soderman et al. 2002). The underlying pathophysiology behind MD remains elusive; prominent theories include decreased endolymph resorption, inner ear vascular abnormalities, autoimmune factors, and an imbalance of water equilibrium in the inner ear (Coelho and Lalwani 2008).

Basement membrane pathology has recently been reported in MD. Our prior study has demonstrated that surgically acquired vestibular endorgans in patients with intractable MD exhibit diffuse basement membrane (BM) thickening, which is significantly correlated to monolayer degeneration of the horizontal cristae ampullaris and caloric paresis (McCall et al. 2009). Mammalian BMs are intertwined networks of

extracellular matrix (ECM) molecules consisting of polymeric laminin and type IV collagen bridged by non-covalent interactions with nidogens and proteoglycans (Kalluri 2003). The mammalian inner ear is rich in BMs, and alterations of the BMs are proposed to mediate the pathology of hearing disorders including Alport's syndrome and presbycusis (Cosgrove et al. 1998; Gratton et al. 2005; Meyer zum Gottesberge and Felix 2005; Sakaguchi et al. 1997; Zehnder et al. 2005).

The BM has been studied extensively in the kidney in which it plays a critical role in solute and ion transport regulation (Tryggvason and Wartiovaaara 2001). Conceivably, BM pathology results in the dysfunctional regulation of endolymphatic fluid and water homeostasis in MD. This has been suggested by the finding of the altered expression of aquaporin-4 and -6 (water channels) in vestibular endorgans from MD patients (Ishiyama et al. 2010).

The immunohistochemical distribution of BM proteins in normal human temporal bones has recently been described; collagen IVα2, laminin-β2, and nidogen-1 colocalize within all human cochlear and vestibular BMs (Ishiyama et al. 2009). These proteins are expressed in the perivascular and perineural BMs in zones demarcating endolymph from perilymph, suggestive of BM involvement in the regulation of water and ionic homeostasis (Ishiyama et al. 2009).

Characterization of the BM and ECM protein expression in the human inner ear might provide clues to the underlying pathophysiology of MD. The most abundant ECM protein in the human inner ear is cochlin, which accounts for 70% of inner ear proteins (Ikezono et al. 2001). Cochlin has been found to colocalize with type II collagen in the same ECM areas of the cochlear duct, cochlea, and vestibule in studies of rat cochleas, suggesting a role for cochlin in cross-linking to type II collagen fibers (Hosokawa et al. 2010; Mizuta et al. 2008). In addition, Nagy et al. (2008) have demonstrated that the second von Willebrand factor A (vWFA)-like domain of cochlin has an affinity for types I, II, and IV collagen. Type II collagen is believed to be responsible for the fibrous structure of the inner ear ECM in order to maintain structural stability in the cochlea and vestibule (Slepecky et al. 1992). Type IV collagen provides the supra-structural foundation of the mammalian BM (Kalluri 2003).

Cochlin, which is the product of the COCH gene, has been associated with the hereditary autosomal dominant form of SNHL, DFNA9 (Khetarpal 2000). DFNA9 deafness is clinically manifested as a progressive audiovestibular dysfunction with adult onset associated with mutations in the cochlin gene, COCH. Inner ear structures in DFNA9 exhibit eosinophilic microfibrillar deposition and severe atrophy of fibrocytes and neural degeneration of the inner ear (Khetarpal 2000; Robertson et al. 2006). Cochlin expression has not been observed in neuroectodermal structures; thus, disruption of the ionic balance of the inner ear secondary to cochlin deposition is hypothesized to occur in the spiral ligament and spiral limbus (Robertson et al. 2006). Additionally, cochlin overexpression has recently been suggested as an etiologic factor in Usher syndrome type 1F, an autosomal dominant syndromic form of audiovestibulopathy (Chance et al. 2010). Based on these findings, a primary or secondary effect on cochlin and BM protein expression and distribution could impair the normal biochemical ionic and fluid homeostasis of the inner ear, resulting in audiovestibular dysfunction.

The present study addresses the hypothesis that cochlin expression is altered in MD patients. We present quantitative immunohistochemical and mRNA analyses of cochlin expression in vestibular endorgans from MD patients compared with control specimens obtained from patients undergoing excision of acoustic neuromas (translabyrinthectomy approach) and autopsy. The distribution of ECM proteins collagen IV, collagen II, laminin-β2, and nidogen-1 in relation to cochlin has also been studied.

Materials and methods

Autopsy specimens The Institutional Review Board (IRB) of UCLA approved this study (IRB approval number 10–001449, approval date 01/08/2012). Appropriate informed consent for inclusion in the study was obtained from each temporal bone donor before death. The temporal bone donors in this study were part of a National Institute of Health (NIH)-funded Human Temporal Bone Consortium for Research Resource Enhancement through the National Institute on Deafness and Other Communication Disorders (NIDCD). The vestibular endorgans were microdissected from one temporal bone from each donor. Human temporal bone specimens were obtained post-mortem from five subjects with a history documenting a lack of auditory or vestibular symptoms (3 female and 2 male with ages ranging from 83 to 98 years old; average age: 87). Post-mortem time ranged from 8 to 12 h. The macula utricli and cristae (horizontal canal cristae) from these patients were used for quantitative immunocytochemistry.

Vestibular endorgans obtained from surgery The utricular maculae and cristae ampullaris were surgically obtained both from patients who had intractable Meniere's disease and who had elected to undergo transmastoid labyrinthectomy and from patients without MD undergoing transmastoid excision of acoustic neuroma. The sensory epithelium was carefully dissected and removed en bloc intraoperatively. All patients had recurrent vertigo spells despite medical management and had non-functional hearing in the operated ear (defined as a word discrimination score of less than 20%). All patients met the 1995 American Academy of Otolaryngology-Head and Neck Foundation criteria for definitive MD (Committee on Hearing

and Equilibrium 1995). The five patients with MD (3 females and 2 males) had ages ranging from 66 to 84 years old (average age: 76). The macula utricle and cristae (horizontal canal cristae) from these patients were used for quantitative immunocytochemistry.

Tissue processing for immunohistochemistry Immediately after surgical removal with regard to MD and acoustic neuroma control specimens and immediately after microdissection with regard to autopsy specimens, the vestibular endorgans were immersed in 4% paraformaldehyde in sodium phosphate buffer (0.11 M, pH 7.4) and kept in this solution for 16 h. Thereafter, the fixative was removed, and the utricles were washed with phosphate-buffered saline solution (PBS; 0.1 M, pH 7.2). Vestibular endorgans from surgery and autopsy were immersed first in 30% sucrose (in PBS) for 3 days and then embedded in Tissue Tek (O.C.T. compound, Polysciences, Warrington, Pa., USA). Cryostat serial sections of 20 μm in thickness were obtained by using a Microm-HM550 Cryostat. The sections were mounted on Superfrost Plus glass slides (Fisher Scientific, Pittsburgh, Pa., USA) and stored at −80 °C until use.

Immunofluorescence staining Cryostat sections were rehydrated with PBS for 10 min and incubated at room temperature for 1 h with a blocking solution containing 1% bovine serum albumin fraction-V (Sigma, St. Louis, Mo., USA) and 1% Triton X-100 (Sigma) in PBS. Next, the solution was removed, and the tissue sections were incubated with cochlin (affinity-purified) goat polyclonal antibody raised against a peptide mapping to the c-terminus of cochlin of human origin (also recognized cochlin from mice and rats; cat. no. D-19, Santa Cruz Biotechnology, Santa Cruz, Calif., USA). On Western blot of mouse eye tissue extract, the antibody gave a single band of approximately 56 kDa. Mouse monoclonal antibodies against collagen IVα2 (1:1000; cat. no. MAB1910; Chemicon, Temecula, Calif., USA), collagen II (1:200; cat. no. sc-59958; Santa Cruz), rabbit polyclonal nidogen-1 (1:500; cat. no. 481918; Calbiochem), and rat monoclonal laminin-β2 (1:250; cat. no. 05–206; Upstate) were also used. Tissue sections were incubated with the relevant primary antibodies overnight at 4°C in a humid chamber. The secondary antibodies against goat IgG and labeled with Alexa 594 and against mouse IgG and labeled with Alexa 494 (1:1000 in PBS; Invitrogen, Carlsbad, Calif., USA) were applied and incubated for 1 h at room temperature in the dark. At the end of the incubation, sections were washed again with PBS and covered with a water-soluble mounting media (Vectashield, Vector Labs, Burlingame, Calif., USA).

Indirect immunocytochemistry Frozen cryostat sections were thawed and washed with PBS, and endogenous peroxidase quenching was performed by incubation for 10 min with 3% hydrogen peroxide (diluted in 100% in methanol). Slides were then washed with PBS for 10 min. Sections were incubated for 1 h with a blocking solution containing 5% normal goat serum (Vector Labs) and 0.5% Triton X-100 (Sigma) in PBS. Incubation with the cochlin antibody was performed for 48 h at 4°C in a humid chamber. The sections were washed with PBS (3×5 min). Next, sections were incubated for 1 h with biotinylated secondary antibody, goat anti-rabbit polyclonal IgG (1:1000, Vector Labs) followed by washes with PBS (3×5 min). Subsequently, incubation was performed for 1 h with Vectastain Elite ABC reagent (Vector Labs) followed by PBS washes (2×5 min). Immunoperoxidase staining was performed by using Immpact DAB (diaminobenzidine) solution (Vector Labs). The reaction was stopped with PBS washes (3×5 min) after 2 min. Slides were mounted with Vectamount AQ aqueous mounting media (Vector Labs) and glass coverslips.

Immunohistochemical controls As positive controls, cryostat sections from mouse inner ear were incubated with cochlin antibodies, and human kidney frozen sections were incubated with antibodies against collagen IV, collagen II, nidogen, and laminin-β2. Inner ear and kidney sections were processed in an identical fashion as human vestibular endorgan sections with regard to fixation time, embedding, sectioning, and immunostaining. As negative controls, vestibular endorgans cryostat sections obtained from surgery or autopsy were stained in the same way without the primary antibody or with antibodies that had been pre-absorbed with the corresponding blocking peptide used to generate the cochlin antibody. Antibody absorption was conducted by incubating the primary antibody with the blocking peptide (1 μg/1 μl). The mixture was then placed at 37°C for 1 h after which time immunohistochemical staining was performed as described above. In both cases, only a faint background in human utricular sections was observed. Both the positive and negative immunohistochemical controls were carried out as previously described (Ishiyama et al. 2009).

Image acquisition Immunostained tissue sections were viewed and imaged with an Olympus BX51 fluorescent microscope (Olympus America, N.Y., USA) equipped with an Olympus DP70 digital camera. The following dichroic mirrors and filters were used: for 4,6-diamidino-2-phenylindole, dichroic mirror (DM) DM40, excitation filter BP330-385, and barrier filter (B) BA420; for Alexa 488, DM505, excitation filter BP470-495, and BA510IF; for Alexa 594, DM570, excitation filter BP530-550, and BA575IF. For bright field, a U-MBF3 mirror was used.

To provide unbiased comparisons of the immunoreactive signal between each specimen, all images were captured by using strictly the same camera settings. Images were

acquired by using MicroSuite Five software (Olympus America). All images were prepared by using the Adobe Photoshop software program run on a Dell Precision 380 computer.

Quantification of immunostained areas Quantitative immunocytochemistry of the cristae and macula utricli cryosections obtained from patients with Meniere's disease or from normal post-mortem patients was performed as described by Ishiyama et al. (2010). To minimize bias in the analysis, the observer was "blinded" to the identity of the tissue samples to be analyzed. A second person not blinded to the sample identity coded each sample. The immunostained area for each cochlin, collagen IV, collagen II, nidogen, and laminin was measured in three different regions of the sensory epithelia. The area immunostained in the crista and utricular macula sections was quantified by using the computer image analysis software ImageJ (available free over the Internet: http://rsb.info.nih.gov/ij/index.html) with the protocol described by Ishiyama et al. (2010). Specifically, we measured the total immunostained area underneath the sensory epithelia, which included the stroma, fibrocytes, and perineural and perivascular membranes and the BM underneath the sensory epithelia.

Statistical analysis For each specimen, mean values of the immunostained area were averaged and subjected to one-way repeated measures analysis of variance (ANOVA) analysis. Comparisons were made between MD and normal post-mortem specimens. Five utricles and five cristae per type of specimen were used for quantification. Values were considered statistically significant at $P \leq 0.05$. Results were expressed as the percentage from the utricles and cristae from normal subjects obtained at autopsy postmortem. The Sigma Stat 3.1 software program (Sigma Stat, Ashburn, Va., USA) was used for statistical analysis.

Considerations with regard to the use of vestibular endorgans obtained from autopsy and surgery for immunohistochemistry Autolytic artifact secondary to fixation delay is unavoidable in human material. This effect is especially critical for examination by cytochemical techniques (Ishiyama et al. 2009). To minimize post-mortem artifacts, temporal bones were harvested between 3 and 9 h post-mortem. In general, shorter post-mortem times are associated with a better signal and a lower background. For the surgical specimens, upon surgical extraction, tissue was immediately fixed and transported to the laboratory, and specimens were post-fixed for 24 h.

Real-time reverse transcription with the polymerase chain reaction For cochlin mRNA expression, the utricular maculae specimens were obtained surgically from three patients with MD (2 males, ages 66 and 77 years old; 1 female, age 60 years old) and three patients undergoing translabyrinthectomy for acoustic neuroma excision (2 males, ages 60 and 73 years old; 1 female, age 59 years old) as controls. Specimens were received into RNAlater (Ambion, Texas) and taken immediately to the laboratory where they were placed overnight at 4°C. The following day, specimens were placed at −80°C until mRNA was extracted.

Total RNA was extracted from each utricle by using TRIzol Reagent (Invitrogene), and reverse transcription (RT) was carried out as described by Ishiyama et al. (2010). The samples were stored at −20°C until use. Amplification was performed with the single-color real-time polymerase chain reaction (PCR) system in a Stratagene Mx3000P (Ishiyama et al. (2010) with cochlin primers (reference sequence accession no. NM_004086; cat. no. PPH08287A), coagulation factor C homolog and cochlin (*Limulus polyphemus*) being validated to ensure amplification of a single product with appropriate efficiency. Samples were run in duplicate, and the amplified products were analyzed by 4% agarose gel electrophoresis.

The threshold cycle (C_t) for each reaction (which was directly related to the amount of starting template in the reaction) was measured within the exponential phase of the PCR by using Stratagene software MxPro V3. Data were normalized by using the housekeeping reference gene D-glyceraldehyde-3-phosphate dehydrogenase (GADPH). A difference in C_t values (DC_t) was then calculated for each gene by taking triplicate C_t values from three reactions and subtracting the mean C_t of the triplicates for the reference gene (GADPH) for each cDNA sample at the same concentration. An additional difference in DC_t value (DDC_t) was calculated for the cochlin gene by taking the triplicate DC_t values for each gene in Meniere's specimens and subtracting the mean DC_t value of the triplicates for acoustic neuroma specimens. The relative expression level was calculated by using the 2^{-DDCt} method (Livak and Schmittgen 2001).

Results

Cochlin immunoreactivity in human vestibular endorgans Figure 1 shows cochlin immunoreactivity (IR) in normal and MD vestibular endorgans. Cochlin-IR was present in the stroma and BM underneath the sensory epithelia of both the crista (Fig. 1a) and the macula utricli (Fig. 1a') in the normal specimens. The supporting cells and hair cells in the sensory epithelia showed no IR. A uniform cochlin-IR signal was seen in all stroma regions of the cristae from the planum semilunatum to the central portion. Figure 1b, b' shows cochlin-IR (low and high magnification, respectively) in the stroma and BM of the maculae utricle from an MD patient. Strong IR was observed in the vestibular

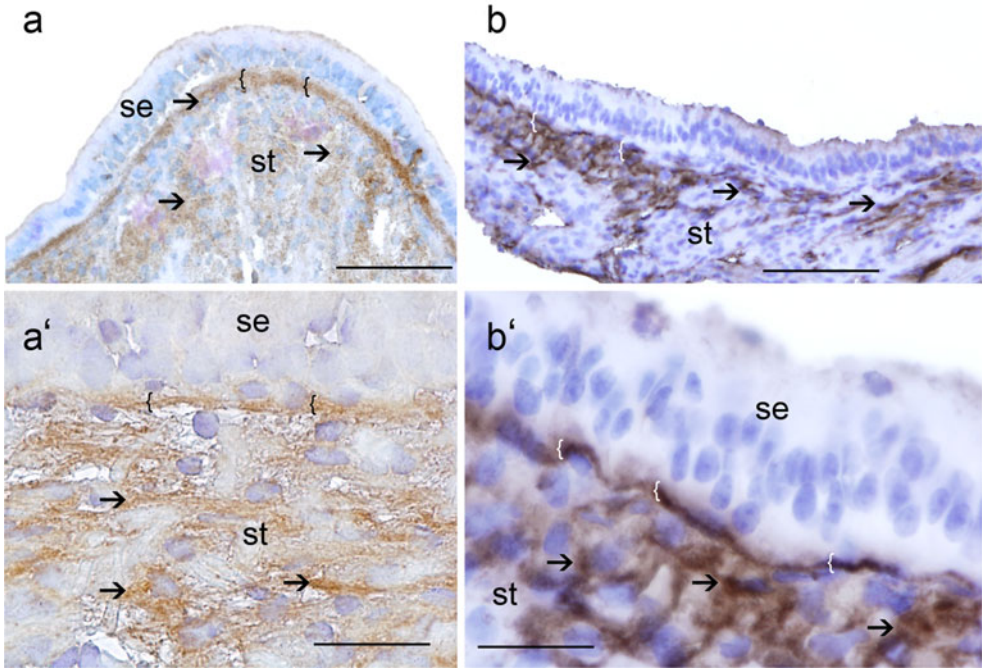

Fig. 1 Cochlin immunoreactivity (IR) in normal and Meniere's disease (MD) vestibular endorgans. **a** Cochlin-IR (*arrows*) was present in the normal crista (autopsy) stroma (*st*) and the basement membrane (BM) (*brackets*) underneath the sensory epithelium (*se*). Supporting cells and hair cells in the sensory epithelium showed no IR. **a'** High magnification view of the normal macula utricle; as in the crista, cochlin-IR is present in the stroma tissue and BM (*brackets*). **b** In MD specimens, strong cochlin-IR (*arrows*) was present in the stroma (*st*) and the BM underneath the sensory epithelium of the macula utricle. **b'** High magnification view of **b**; strong cochlin-IR is seen in the BM (*brackets*) and stroma (*arrows*). Hematoxylin counterstaining. *Bars* 100 μm (**a**, **b**), 25 μm (**a'**, **b'**)

endorgans of patients when compared with that in normal specimens. These findings were consistent in every MD specimen analyzed.

Cochlin mRNA expression in human vestibular endorgans Isolated mRNA was subjected to real-time RT-PCR to detect the mRNA of cochlin. A comparison of cochlin mRNA expression levels between MD and control (acoustic neuroma) specimens showed a 36% increase in cochlin mRNA expression from the MD cristae (Fig. 2a). The RT-PCR amplified cochlin mRNA products from MD and control specimens (AN) showed bands, on electrophoresis, between 150 and 200 bp consistent with the established cochlin mRNA length (Fig. 2b).

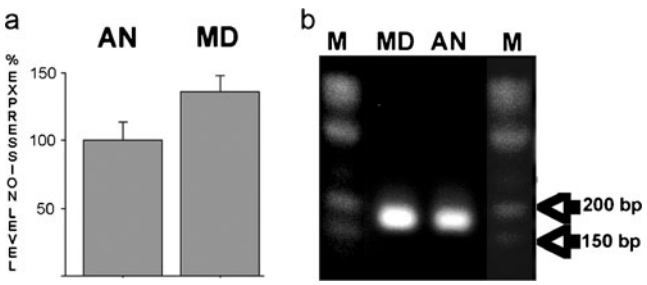

Fig. 2 Cochlin mRNA expression in MD. **a** COCH expression in MD versus control (acoustic neuroma, *AN*) specimens. Data represent the mean ± SD of the three MD and three control cristae. **b** RT-PCR products of COCH amplified from MD and AN patients. Molecular size markers (*M*) are indicated (ladder amplicon sizes of 150 bp and 200 bp)

Colocalization of cochlin and collagen IV Cochlin immunofluorescence (IF) was also examined in both control specimens from postmortem normal subjects and MD vestibular endorgans obtained from ablative surgery. In the normal crista ampullaris, cochlin-IF appeared as a fine punctate reaction in the stroma and blood vessels (Fig. 3a). MD crista ampullaris (Fig. 3b) exhibited an increase in cochlin-IF in the stroma and BM underneath the sensory epithelia. Collagen-IV-IF in the normal crista was present in perivascular BM and in the BM underneath the sensory epithelia (Fig. 3c). In the cristae from MD specimens, collagen-IV-IF was decreased in the BM (Fig. 3d) but not in perivascular and perineural BM. Figure 3e, f shows merged images from normal (Fig. 3a, c) and MD crista (Fig. 3b, d), respectively.

In the normal macula utricli, cochlin-IF appeared as a fine punctate reaction in the stroma and blood vessels (Fig. 4a). In the MD utricle, an increase was observed in cochlin-IF in the stroma and BM underneath the sensory epithelia (Fig. 4b). Collagen-IV-IF in the normal utricle was present in perivascular BM and in the BM underneath the

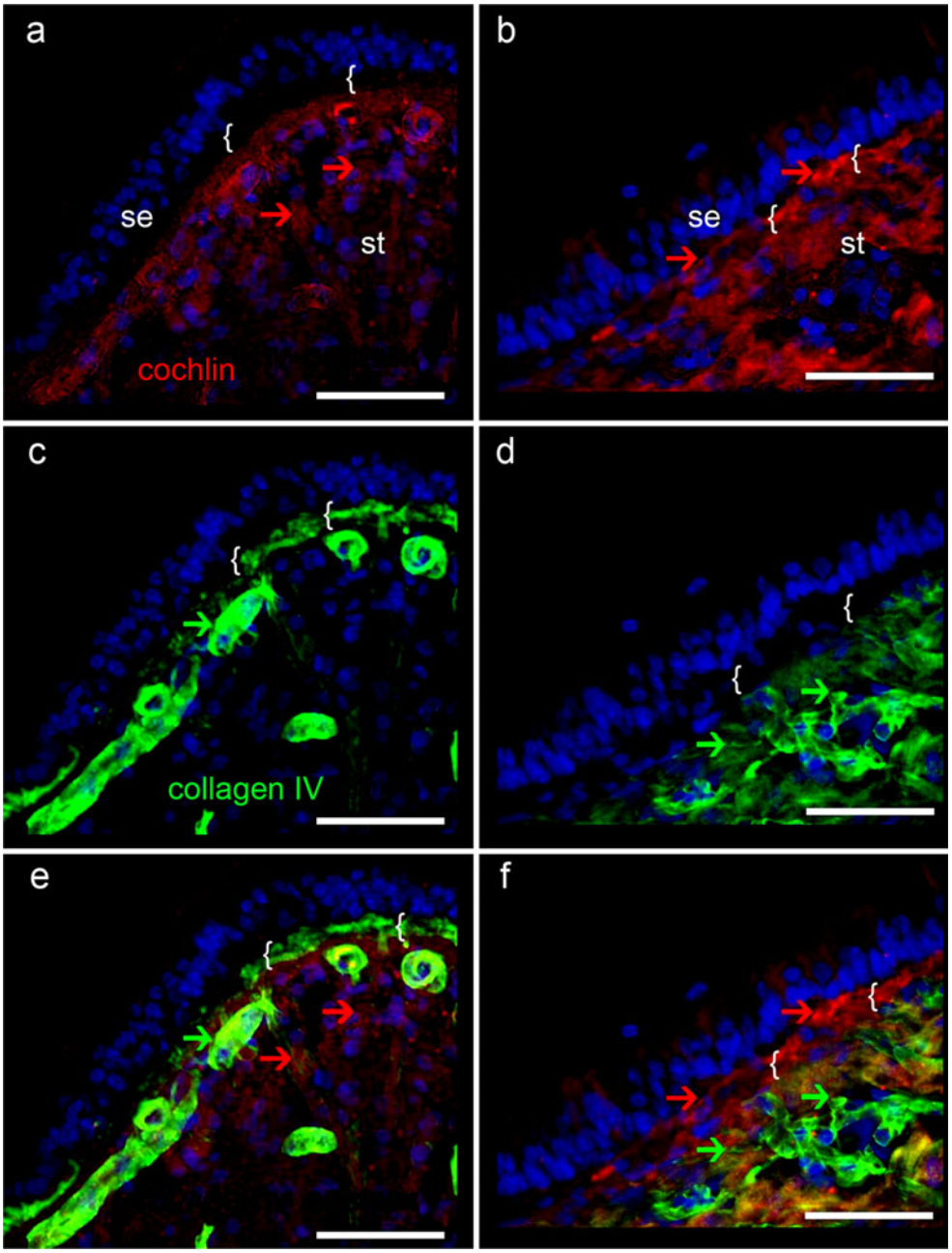

Fig. 3 Cochlin and collagen IV immunofluorescence (IF) in normal and MD crista. **a** Cochlin-IF in normal crista (*red*) appears as a fine punctate reaction in the stroma (*st*, *arrows*). **c** Collagen-IV-IF (*green arrows*) in a similar section as in **a**. Collagen IV is present in perivascular BM and in the BM (*brackets*) underneath the sensory epithelium (*se*). **b** Cochlin-IF from an MD crista with increased cochlin-IF (*red*) in the BM underneath the sensory epithelium (*brackets*) and stroma. **d** Collagen-IV-IF is decreased in the BM but not in the stroma. The sensory epithelium was not immunoreactive. **e**, **f** Merged images of **a**, **c** and of **b**, **d**, respectively. *Blue* DAPI (4,6-diamidino-2-phenylindole) staining of cell nuclei. *Bars* 60 μm

sensory epithelia (Fig. 4c). In contrast, in the utricle from MD specimens, collagen-IV-IF was decreased in both perivascular and perineural BM (Fig. 3d). Figure 4e, f show merged images from the normal (Fig. 4a, c) and MD utricle (Fig. 4b, d), respectively.

Cochlin and laminin-β2-IF Figure 5a shows cochlin-IF in the normal utricle. In MD utricle, an increase occurred in cochlin-IF in the stroma and BM underneath the sensory epithelia (Fig. 5b). Laminin-β2-IF was present in perivascular BM and in the BM underneath the sensory epithelia in the normal utricle (Fig. 5c). In contrast, in the utricle from MD specimens, laminin-β2-IF was decreased the BM underneath the sensory epithelia and to a lesser extent in perivascular and perineural BM (Fig. 5d). Figure 5e, f are merged images from the normal (Fig. 5a, c) and MD utricle (Fig. 5b, d), respectively. The cristae ampullaris from MD patients presented a similar decrease in laminin-β2-IF (not shown).

Collagen-II-IF and nidogen-1-IF In the normal crista and utricle, collagen-II-IF and nidogen-IF was localized in perivascular and perivascular BMs and BM underneath the sensory epithelium, thus resembling the distribution of collagen IV. In MD vestibular endorgans, collagen II and nidogen immunostaining was unchanged when compared with that of the normal vestibular endorgans (not shown).

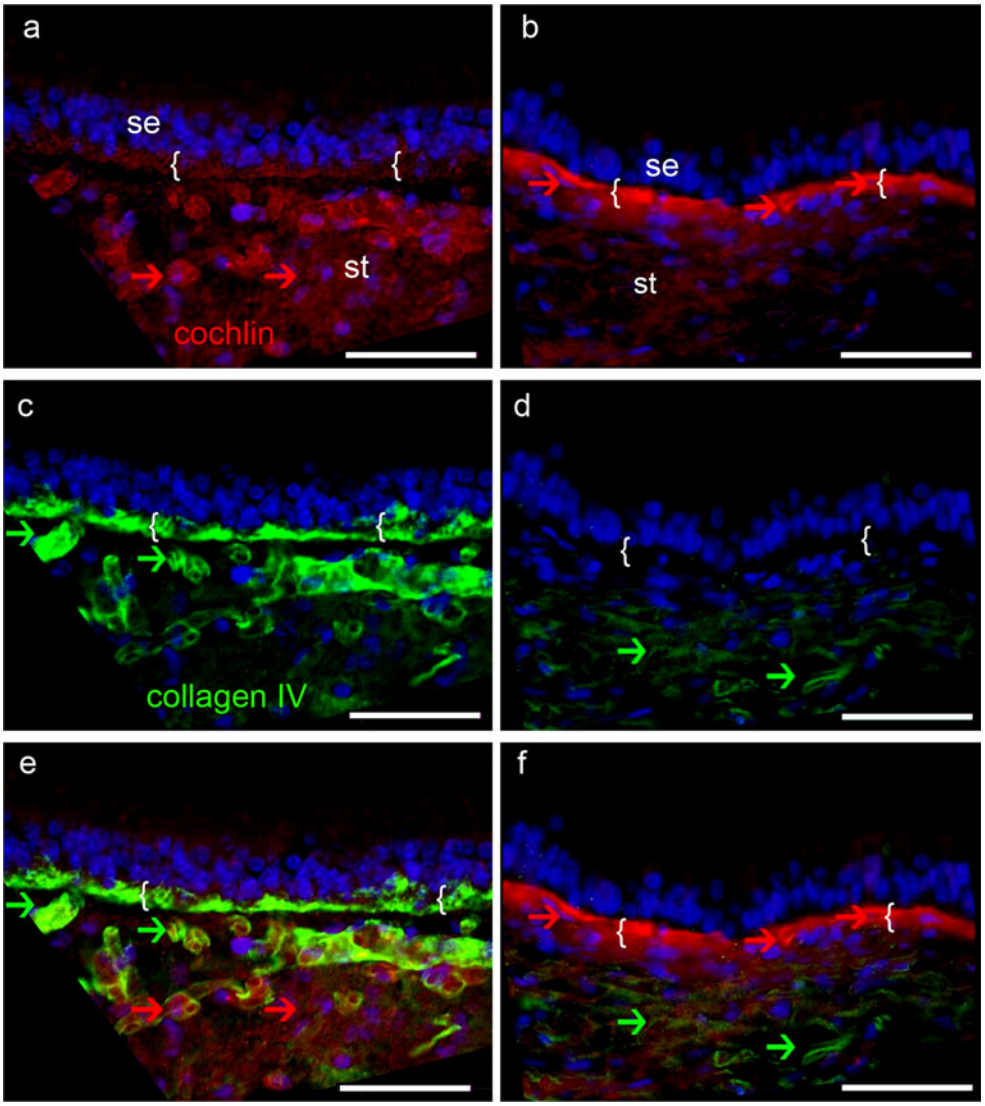

Fig. 4 Cochlin-IF and collagen-IV-IF in normal and MD utricle. **a** Cochlin-IF in the normal utricle stroma (*red*, *arrows*). **c** Collagen-IV-IF (*green arrows*) in a similar section as in **a**. Collagen IV is present in perivascular BM and in the BM (*brackets*) underneath the utricle sensory epithelium (*se*). **b** Cochlin-IF from an MD utricle with increased cochlin-IF in the BM (*brackets*) and stroma (*st*). **d** Collagen-IV-IF (*green arrows*) is decreased in both the BM underneath the sensory epithelium and the stroma. **e**, **f** Merged images of **a**, **c** and of **b**, **d**, respectively. *Blue* DAPI staining of cell nuclei. *Bars* 60 μm

Quantitative immunocytochemistry Quantitative IF measurements for cochlin showed statistically significant increased cochlin IR from the cristae and utricle from subjects with MD compared with those from normal autopsy subjects (Fig. 6). Changes in collagen IV were statistically significantly decreased in MD cristae and utricle when compared with the normal vestibular endorgans (Fig. 6). Laminin-β2-IF was statistically significantly decreased in MD cristae and utricle when compared with the normal vestibular endorgans (Fig. 6). In contrast, no statistically significant changes were observed in collagen-II-IF and nidogen-IF in MD specimens when compared with normal specimens.

Cochlin-IR controls Positive controls for the cochlin antibodies were tested in mice cochlea (Fig. 7a) and vestibular endorgans (Fig. 7b). Immunoreactive signal was detected in the spiral ligament and stroma of the macula utricle of the mouse. Negative controls (human vestibular endorgans incubated with normal serum or no primary antibody) exhibited no IR within the vestibular (Fig. 7c) or mouse cochlear (Fig. 7d) tissues. Positive and negative controls for collagen IV, collagen II, nidogen-1, and laminin-β2 were conducted as previously described (Ishiyama et al. 2010).

Discussion

In the present study, we describe the protein immunolocalization and mRNA expression of cochlin and the immunolocalization of other ECM proteins in the vestibular endorgans from patients diagnosed with MD and compare the cochlin expression in MD patients with that in normal human vestibular endorgans. Both immunolocalization and mRNA expression show increased levels of cochlin deposition and mRNA expression in the BMs of the cristae ampullaris and maculae utricli in subjects with MD. In addition, a

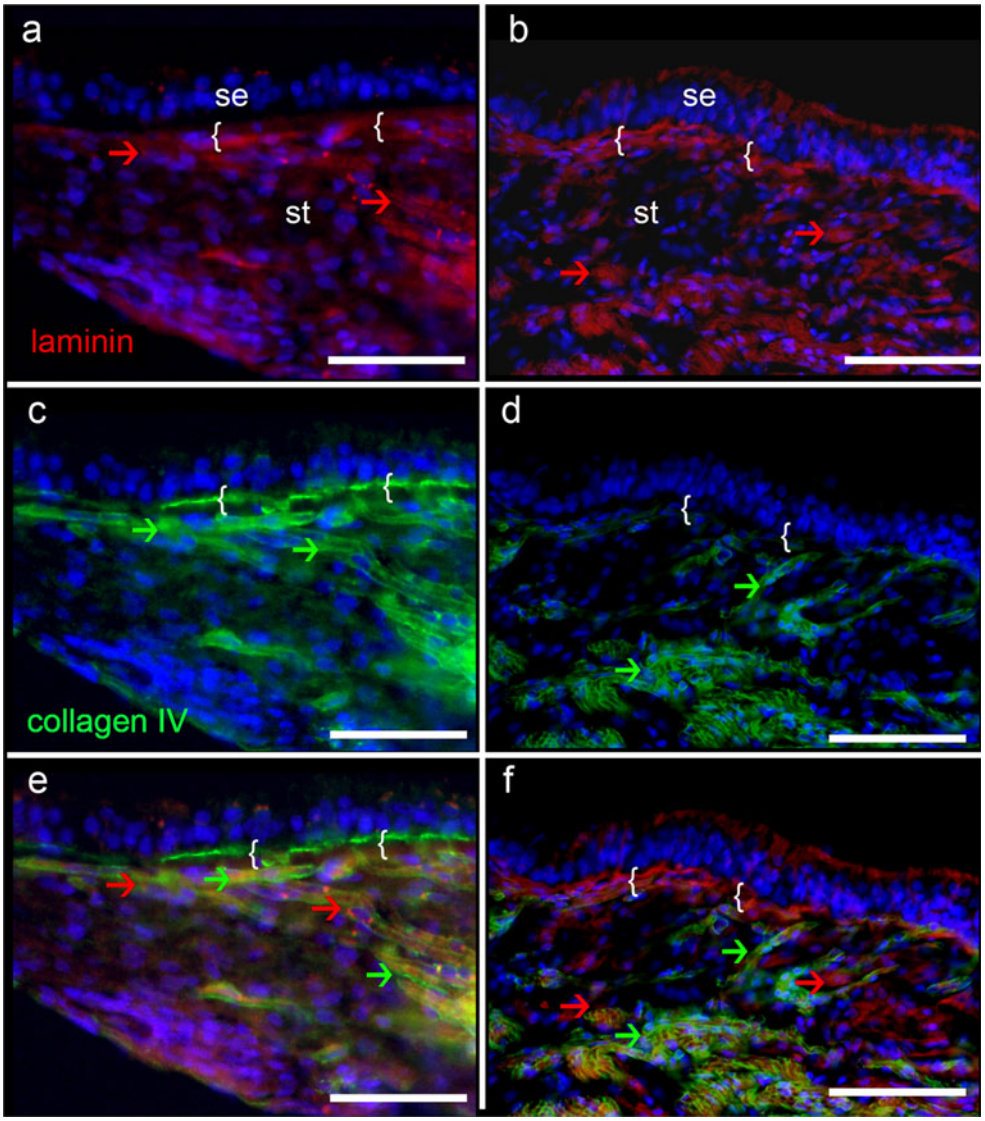

Fig. 5 Cochlin-IF and laminin-β2-IF. **a** Cochlin-IF in the normal utricle stroma (*red*, *arrows*). **c** Laminin-β2-IF (*green arrows*) in a similar section as in **a**. Laminin-β2-IF is present in perivascular BM and in the BM (*brackets*) underneath the utricle sensory epithelium (*se*). **b** Cochlin-IF from an MD utricle in the BM (*brackets*) and stroma (*st*). **d** Laminin-β2-IF is decreased in both the BM underneath the sensory epithelium and the stroma. **e**, **f** Merged images of **a**, **c** and of **b**, **d**, respectively. *Blue* DAPI staining of cell nuclei. *Bars* 55 μm

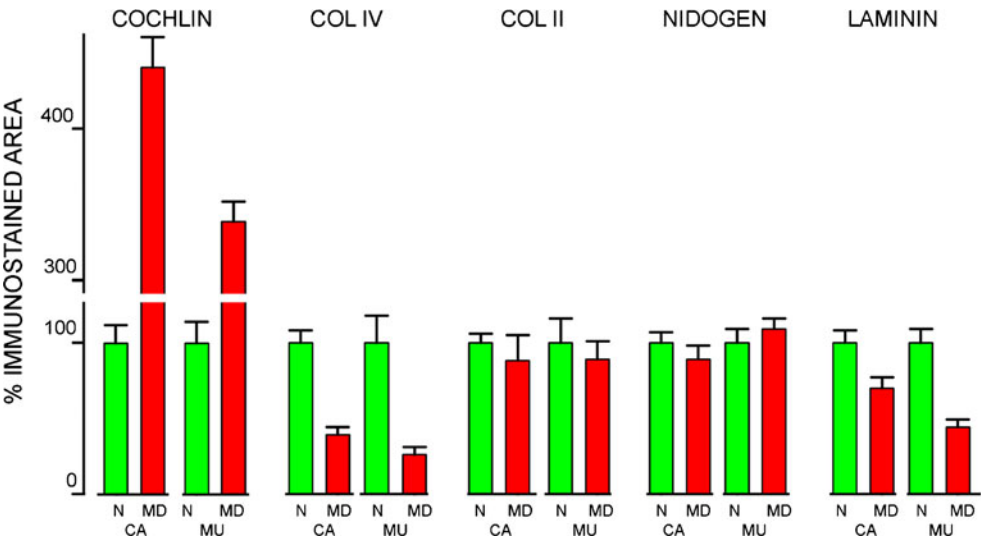

Fig. 6 Quantitative comparison of cochlin-, collagen-IV- (*COLIV*), collagen-II- (*COLII*), nidogen-, and laminin-IR between autopsy (*green*) and MD (*red*) specimens. Cochlin-IR reveals statistically significant changes between MD (increase IR) and normal (*N*) crista (*CA*) and utricle (*MA*). Collagen-IV-IR and laminin-IR were statistically significantly decreased. Collagen-II-IR and nidogen-IR showed no significant differences

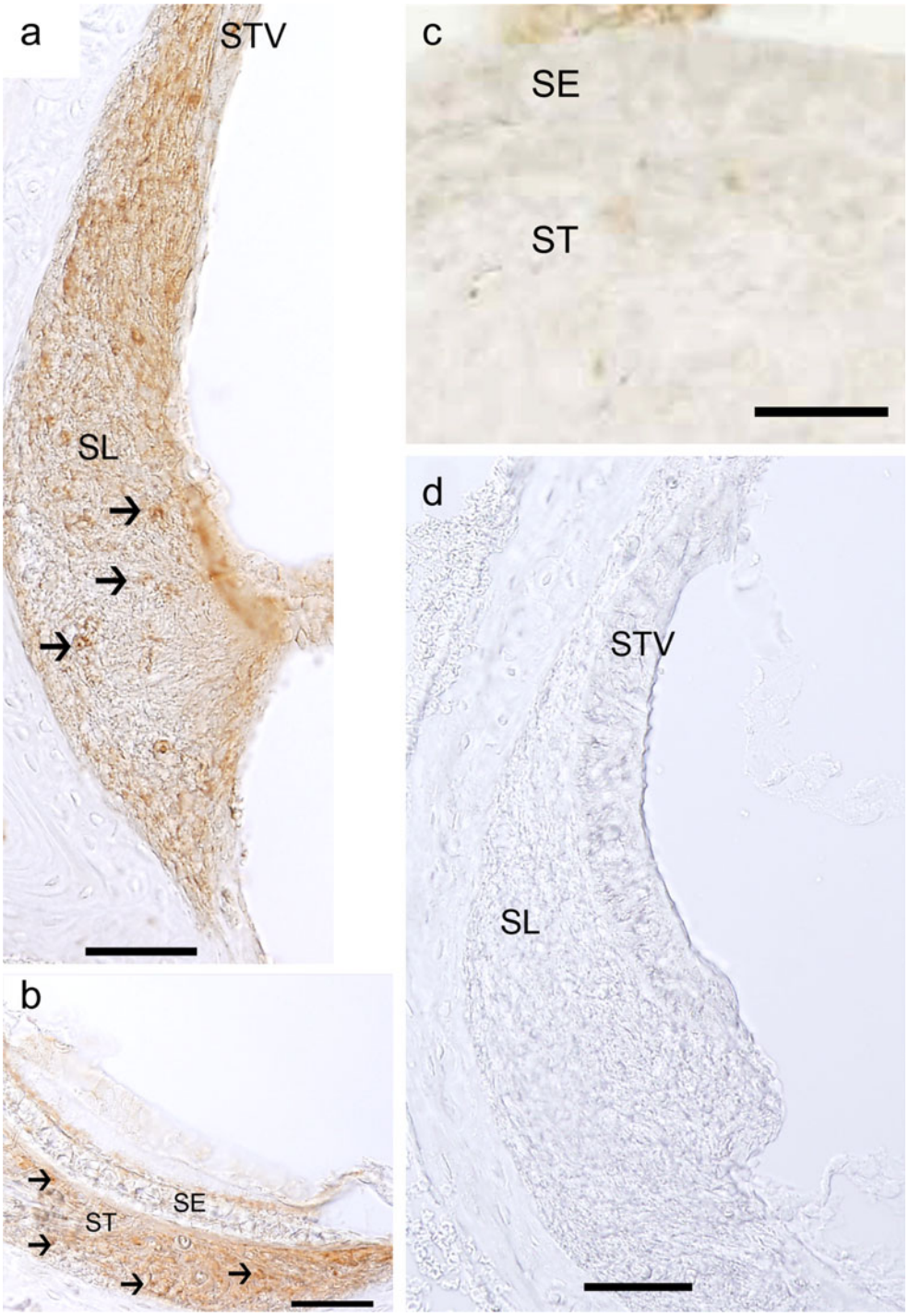

Fig. 7 Cochlin-IR controls. **a**, **b** Positive controls (*arrows* positive immunostaining). **a** Cochlin-IR in mouse cochlea spiral ligament (*SL* spiral ligament, *STV* stria vascularis). **b** Cochlin-IR in the mouse macula utricli (*SE* sensory epithelium, *St* stroma). **c**, **d** Negative controls. **c** Cross section of human utricle immunostained with all reagents except for the cochlin antibody; no specific reaction was observed. **d** No IR in the mouse cochlea was detected when the primary antibody was omitted. *Bars* 35 μm (**a**, **b**, **d**), 25 μm (**c**)

significant decrease has been seen in collagen IV and laminin-β2 in MD specimens, whereas collagen II and nidogen-1 remain unchanged.

Increased cochlin expression in human MD specimens Cochlin, the major ECM protein in the human inner ear, is associated with the autosomal dominant form of adult-onset SNHL and vestibular symptoms, known as DFNA9 (Ikezono et al. 2001; Robertson et al. 1998). DFNA9 has a similarity in clinical symptomatology to MD (Fransen et al. 1999). Patients with DFNA9 typically manifest with progressive SNHL starting between the third and sixth decade with accompanying vestibular symptoms. Despite the likelihood that the specific COCH mutations causing DFNA9 audiovestibulopathy are not responsible for sporadic MD (Sanchez et al. 2003; Usami et al. 2003), our data demonstrate cochlin

overexpression in the vestibular endorgans of the subjects with intractable MD.

The function of cochlin in the inner ear has largely been studied, with reference to DFNA9, as the largest component of the inner ear ECM. Mature cochlin is a modular polypeptide consisting of a LCCL domain and two vWFA-like domains, which are found primarily in proteins in the ECM (Colombatti and Bonaldo 1991). Immunohistochemical analysis of human and rodent fetal ears and adult rodent ears has shown cochlin expression in the same areas as those exhibiting type II collagen (Goodyear and Richardson 2002; Khetarpal et al. 1994; Tsuprun and Santi 1999). In the rat vestibular organ, cochlin is expressed in the stroma of the maculae of the otolithic organs and the cristae ampullares and in channels that lie in the bony labyrinth and that transmit dendritic innervation to the cristae and maculae, similar to our postmortem normal specimens (Ikezono et al. 2005). COCH mRNA expression has also been detected, histologically by in situ hybridization, in the stromal cells underlying the sensory epithelium in the crista ampullaris (Robertson et al. 2001).

The role of cochlin and the etiology of DFNA9 have been recently studied by using a cochlin knock-out ($Coch^{-/-}$) and a knock-in ($Coch^{+/+}$) mouse model (Jones et al. 2011). Both mouse models show elevated auditory brain responses (ABRs) at 21 months of age. The $Coch^{-/-}$ model exhibits changes at the highest frequency, and the $Coch^{+/+}$ model demonstrates changes at all frequencies. The heterozygous knock-in mouse model shows elevated ABRs similar to those of homozygotes. Vestibular evoked potentials are elevated in the $Coch^{-/-}$ model at 13 and 21 months and as early as 7 months in the $Coch^{+/+}$ model. These results indicate that, in both mouse models, vestibular function is compromised before cochlear function (Jones et al. 2011). Morphological examination of the $Coch^{-/-}$ and the $Coch^{+/+}$ mice has not revealed any significant histological changes. These results suggest that the pathology is attributable to events occurring at the molecular level.

Collagen IV and laminin-β2 expression are decreased, whereas collagen II and nidogen remain unchanged in MD specimens Cochlin is upregulated in the vestibular endorgans of MD patients, whereas collagen IV and laminin expression is significantly decreased. Our presented data showing a marked increase in cochlin expression and an associated decrease in collagen IV and laminin expression lend support to BM pathophysiology in MD. Studies of the inner ear ECM suggest a structural role for cochlin.

Our study does not show alterations in collagen II expression in the vestibular endorgans of MD subjects. The eosinophilic deposits containing cochlin in DFNA9 are associated with a decreased expression of type II collagen, suggesting a direct effect of the mutated cochlin or altered binding of cochlin with the fibrillar collagens (Robertson et al. 2001). In studies of glaucoma, increased cochlin expression follows disease progression and also parallels a decrease in type II collagen, suggesting altered tissue architecture leading to an obstruction in the aqueous flow in the eye (Bhattacharya et al. 2005a, b). Another study has employed electron microscopy to examine DFNA9 temporal bone sections and shown that normal collagen fibrillogenesis is disrupted by excess microfibrillar substance, resulting in the degradation of collagens and ECM components (Khetarpal 2000). Like collagen II, nidogen expression is not unaltered in vestibular endorgans from subjects with MD.

Altered ECM protein expression in MD We propose that altered cochlin and ECM protein expression might play a role in MD. Given that endolymphatic hydrops is the most consistent temporal bone finding associated with MD, a disruption in water and ion homeostasis in the inner ear via ECM protein alteration probably contributes to the underlying physiology of the disease. ECM molecules are thought to regulate extracellular ion homeostasis and fluid filtration (Eikmans et al. 2003). Our prior work analyzing the histopathology and ultrastructure of vestibular endorgans in patients with intractable MD has revealed BM thickening, which correlates with neuroepithelial degeneration (McCall et al. 2009).

This study is unique in its analysis of the cochlin expression in individual vestibular endorgans from human patients with active MD. At the time of surgery, these patients exhibited active disease, i.e., recent vertigo spells that were unresponsive to medical therapy. Therefore, they were in an active disease state at the time of surgery. The severity of the disease appeared to be generated from the endorgans as the vast majority of patients undergoing ablative labyrinthectomy (surgical removal of the endorgans) clinically improved postoperatively. Given the complex interaction of cochlin with other ECM proteins in the human vestibular endorgans, further studies are therefore necessary to elucidate the role of cochlin in the pathophysiology of MD. Notably, several types of cochlin isoforms have been detected in the inner ear (Sekine et al. 2010); thus, changes in protein expression may be heterogeneous, with the current study identifying only one type of cochlin. Further studies investigating other cochlin isoforms are indicated.

In conclusion, an increase in cochlin expression occurs in the BMs of vestibular endorgans from subjects with MD, together with a marked decrease in collagen IV and laminin-β2 expression in these MD patients. Cochlin appears to be structurally important in BM physiology, and its upregulation might contribute to the dysfunctional inner ear homeostasis underlying the pathophysiology of MD.

References

Baloh RW (2001) Prosper Meniere and his disease. Arch Neurol 258:151–156

Bhattacharya SK, Annangudi SP, Salomon RG, Kuchtey RW, Peachey NS, Crabb JW (2005a) Cochlin deposits in the trabecular meshwork of the glaucomatous DBA/2J mouse. Exp Eye Res 80:741–744

Bhattacharya SK, Rockwood EJ, Smith SD, Bonilha VL, Crabb JS, Kuchtey RW, Robertson GN, Peachey NS, Morton CC, Crabb JW (2005b) Proteomics reveal cochlin deposits associated with glaucomatous trabecular meshwork. J Biol Chem 280:6080–6084

Chance MR, Chang J, Liu S, Gokulrangan G, Chen DH, Lindsay A, Gen R, Zhen QY, Alagramam K (2010) Proteomics, bioinformatics and targeted gene expression analysis reveals up-regulation of cochlin and identifies other potential biomarkers in the mouse model for deafness in Usher syndrome type 1F. Hum Mol Genet 19:1515–1527

Coelho DH, Lalwani AK (2008) Medical management of Meniere's disease. Laryngoscope 118:1099–1108

Colombatti A, Bonaldo P (1991) The superfamily of proteins with von Willebrand factor type A-like domains: one theme common to components of extracellular matrix, hemostasis, cellular adhesion, and defense mechanisms. Blood 77:2305–2315

Committee on Hearing and Equilibrium (1995) Committee on Hearing and Equilibrium guidelines for the diagnosis and evaluation of therapy in Menière's disease. American Academy of Otolaryngology-Head and Neck Foundation. Otolaryngol Head Neck Surg 113:181–185

Cosgrove D, Samuelson G, Meehan DT, Miller C, McGee J, Walsh EJ, Siegel M (1998) Ultrastructual, physiological, and molecular defects in the inner ear of a gene-knockout mouse model for autosomal Alport syndrome. Hear Res 121:84–98

Eikmans M, Baelde JJ, Heer E de, Bruijn JA (2003) Extracellular matrix homeostasis in renal diseases: a genomic approach. J Pathol 200:526–536

Fransen E, Verstreken M, Verhagen WI, Fl W, Huygen PL, D'Haese P, Robertson NG, Morton CC, McGuirt WT, Smith RJ, Declau F, Van de Heyning PH, Van Cam G (1999) High prevalence of symptoms of Meniere's disease in three families with a mutation in the COCH gene. Hum Mol Genet 8:1425–1429

Goodyear RJ, Richardson GP (2002) Extracellular matrices associated with the apical surfaces of sensory epithelia in the inner ear: molecular and structural diversity. J Neurobiol 53:212–227

Gratton MA, Rao VH, Meehan DT, Askew C, Cosgrove D (2005) Matrix metalloproteinase dysregulation in the stria vascularis of mice with Alport syndrome: implications for capillary basement membrane pathology. Am J Pathol 166:1465–1474

Hosokawa S, Mizuta K, Nakanishi H, Hashimoto Y, Arai M, Mineta H, Shindo S, Ikezono T (2010) Ultrastructural localization of cochlin in the rat cochlear duct. Audiol Neuro Otol 15:247–253

Ikezono T, Omori A, Ichinose S, Pawankar R, Watanabe A, Yagi T (2001) Identification of the protein product of the Coch gene (hereditary deafness gene) as the major component of bovine inner ear protein. Biochem Biophys Acta 1535:258–265

Ikezono T, Shindo S, Ishizaki L, Li L, Tomiyama S, Takumida M, Pawankar R, Watanabe A, Saito A, Yagi T (2005) Expression of cochlin in the vestibular endorgans of rats. ORL J Otolaryngol Relat Spec 67:252–258

Ishiyama A, Mowry SE, Lopez IA, Ishiyama G (2009) Immunohistochemical distribution of basement membrane proteins in the human inner ear from older subjects. Hear Res 254:1–14

Ishiyama G, Lopez IA, Beltran-Parrazal L, Ishiyama A (2010) Immunohistochemical localization and mRNA expression of aquaporins in the macula utriculi of patients with Meniere's disease and acoustic neuroma. Cell Tissue Res 340:407–419

Jones SM, Robertson NG, Given S, Giersh BS, Liberman MC, Morton CC (2011) Hearing and vestibular deficits in the Coch$^{-/-}$ null mouse model: comparison to the Cochg88E/G88E mouse and to DFNA9 hearing and balance disorder. Hear Res 272:42–48

Kalluri R (2003) Basement membranes: structure, assembly and role in tumor angiogenesis. Nat Rev Cancer 3:422–433

Khetarpal U (2000) DFNA9 is a progressive audiovestibular dysfunction with a microfibrillar deposit in the inner ear. Laryngoscope 110:1379–1384

Khetarpal U, Robertson NG, Yoo TJ, Morton CC (1994) Expression and localization COL2A1 mRNA and type II collagen in human fetal cochlea. Hear Res 79:59–73

Livak KJ, Schmittgen TD (2001) Analysis of relative gene expression data using real time quantitative PCR and the 2(−Delta Delta C (T)) method. Methods 25:402–408

McCall A, Ishiyama G, Lopez IA, Bhuta S, Vetter S, Ishiyama A (2009) Histopathological and ultrastructural analysis of vestibular endorgans obtained from patients with Meniere's disease. BMC Ear Nose Throat Disord 9:4

Meyer zum Gottesberge AM, Felix H (2005) Abnormal basement membrane in the inner ear and the kidney of the Mpv17$^{-/-}$ mouse strain: ultrastructural and immunohistochemical investigations. Histochem Cell Biol 124:507–516

Mizuta K, Ikezono T, Iwasaki S, Arai M, Hashimoto Y, Pawankar R, Watanabe T, Shindo S, Mineta H (2008) Ultrastructural co-localization of cochlin and type II collagen in the rat semicircular canal. Neurosci Lett 434:104–107

Nagy I, Trexler M, Patthy L (2008) The second von Willebrand type A domain of cochlin has high affinity for type I, type II and type IV collagens. FEBS Lett 582:4003–4007

Robertson NG, Lu L, Heller S, Merchant SN, Eavey RD, McKenna M, Nadol JB Jr, Miyamoto RT, Linthicum FH Jr, Lubianca Nerto JF, Hudspeth AJ, Seidman CE, Morton CC, Seidman JG (1998) Mutations in a novel cochlear gene cause DFNA9, a human non-syndromic sensorineural deafness with vestibular dysfunction. Nat Genet 20:299–303

Robertson NG, Resendes BL, Lin JS, Lee C, Aster JC, Adams JC, Morton CC (2001) Inner ear localization of mRNA and protein products of COCH, mutated in the sensorineural deafness and vestibular disorder, DFNA9. Hum Mol Genet 10:2493–2500

Robertson NG, Cremers C, Huygen PL, Ikezono T, Krastins B, Kremer H, Kuo SF, Liberman MC, Merchant SN, Miller CE, Nadol JB Jr, Sarracino DA, Verhagen WI, Morton CC (2006) Cochlin immunostaining of inner ear pathologic deposits and proteomic analysis in DFNA9 deafness and vestibular dysfunction. Hum Mol Genet 15:1071–1085

Sakaguchi N, Spicer SS, Thomopoulos GN, Schulte BA (1997) Increased laminin deposition in capillaries of the stria vascularis of quiet-aged gerbils. Hear Res 105:44–56

Sanchez E, Lopez-Escamez JA, Lopez-Nevot MA, Lopez-Nevot A, Cortes R, Martin J (2003) Absence of COCH mutations in patients with Meniere disease. Eur J Hum Genet 11:744–748

Sekine K, Ikezono T, Matsumura T, Shindo S, Watanabe A, Li L, Pawankar R, Nishino T, Yagi T (2010) Expression of cochlin mRNA splice variants in the inner ear. Audiol Neurootol 15:88–96

Slepecky NB, Savage JE, Yoo TJ (1992) Localization of type II, IX, and V collagen in the inner ear. Acta Otolaryngol 112:611–617

Soderman AC, Bagger-Sjoback D, Bergenius J, Langius A (2002) Factors influencing quality of life in patients with Meniere's disease, identified by a multidimensional approach. Otol Neurotol 23:941–948

Tryggvason K, Wartiovaaara J (2001) Molecular basis of glomerular permselectivity. Curr Opin Nephrol Hypertens 10:534–549

Tsuprun V, Santi P (1999) Ultrastructure and immunohistochemical identification of the extracellular matrix of the chinchilla cochlea. Hear Res 129:35–49

Usami S, Takahashi K, Yuge I, Ohtsuka A, Namba A, Abe S, Fransen E, Patthy L, Otting G, Van Camp G (2003) Mutations in the COCH gene are a frequent cause of autosomal dominant progressive cochleovestibular dysfunction, but not of Meniere's disease. Eur J Hum Genet 11:744–748

Zehnder A, Adams J, Santi PA, Kristiansen AG, Wacharasindhu C, Mann S, Kalluri R, Gregory MC, Kashtan CE, Merchant SN (2005) Distribution of type IV collagen in the cochlea in Alport's syndrome. Arch Otolaryngol Head Neck Surg 131:1007–1113